

Influences of coarse grid selection on Kirchhoff beam migration

LI Jiabin¹, SUN Hui^{1,2,*}, ZHANG Zhihou¹, HAN Fuxing³ and LIU Minchen³

1. Faculty of Geosciences and Environmental Engineering, Southwest Jiaotong University, Chengdu 611756, China;

2. School of Resources and Environment, University of Electronic Science and Technology of China, Chengdu 611731, China;

3. College of Geo-Exploration Science and Technology, Jilin University, Changchun 130026, China

Abstract: Kirchhoff beam migration is a beam migration method, which focuses on rapid imaging of geological structures. Although this imaging method ignores the amplitude information in the calculation process, it can calculate multi-arrival traveltime. This migration method takes into account both imaging accuracy and computational efficiency. Kirchhoff beam migration employs coarse grid techniques in several key steps such as traveltime calculation, weight function calculation, and imaging calculation. The selection of the coarse mesh size has an important influence on the computational efficiency and imaging accuracy of the migration imaging method. This paper will analyze this influence and illustrate the analysis results by the Marmousi data sets.

Keywords: Kirchhoff beam migration; prestack depth migration; coarse grid selection; beam propagator; traveltime calculation

0 Introduction

Kirchhoff migration and beam migration are two methods for ray-type prestack depth migration. The former uses the Kirchhoff integral to express the seismic wave field, whereas the latter simultaneously migrates multiple seismic traces, which can be seen as an improvement of the Kirchhoff migration. Kirchhoff beam migration discussed in this paper is one of the beam migration methods.

Kirchhoff theory first appeared in the field of aperture diffraction in optics, and was later applied to the seismic exploration (Hagedoorn, 1954; French, 1975; Schneider, 1978). The Kirchhoff migration originates from the diffraction stack migration, but is different from the diffraction stack migration method.

The theoretical basis of diffraction stack method is geometric seismology, which only retains the kinematic characteristics of seismic waves. While the Kirchhoff migration method uses Kirchhoff integral to solve the wave equation, and thus realizes the wave field continuation and migration imaging of seismic waves. The process of Kirchhoff migration not only acquires the kinematic characteristics of seismic waves, but also acquires the dynamic parameters of seismic waves. Thus, Kirchhoff migration has the advantage of high efficiency and stability.

Seismic wave traveltime is an important factor of the imaging effect and computational efficiency for Kirchhoff migration. Kirchhoff migration can be divided into single-arrival method and multi-arrival method according to the traveltime type. Although the migra-

tion results of different single-arrival methods are different, the Kirchhoff migration method will miss the migration energy carried by other traveltimes if only one single traveltime is calculated, and the result of the migration method is difficult to meet the high-precision imaging requirements. Some scholars have proposed the multi-arrival Kirchhoff migration methods (Xu & Lambare, 2004; Xu *et al.*, 2004) to solve the problem. Multi-arrival Kirchhoff migration method has high imaging accuracy, which is similar to that of the differential methods. However, the shortcomings of this method are also very prominent, in the implementation process, it is necessary to calculate large number of rays, which lead to a decline in computational efficiency. Although many scholars have selected the traveltime in the migration algorithm, it still cannot completely solve this problem.

In seismic exploration, Červený *et al.* (1982) first adopted Gaussian beams to calculate seismic wave fields. Based on this method, Hill (1990) proposed a Gaussian beam poststack migration method, which decomposes the seismic data in the window into plane waves in different directions by local slant stack, and images each plane wave. Hill's selection methods of key parameters such as the window spacing, initial beamwidth and ray sampling density are important for the later beam migration method. Hale (1992) compared the advantages and disadvantages of the Kirchhoff migration, slant stack migration and Gaussian beam migration methods and gave some implementation techniques for Gaussian beam migration, including how to apply coarse grid technique and choose the nearest point. Sun *et al.* (2000) introduced the beam algorithm into Kirchhoff migration and proposed Kirchhoff beam migration.

Hill (2001) extended the method of Gaussian beam migration to a prestack method, using the steepest descent method to simplify the imaging formula to improve the computational efficiency. Nowack (2003) and Gray (2005) extended the Gaussian beam prestack depth migration to a common shot domain algorithm based on Hill's method. Liu and Pala-

charla (2011) proposed a simplified Kirchhoff beam migration, in which only the kinematic ray tracing equations are solved, and the analytical formula derived from the uniform medium is used instead of the wavefront curvature. Using the analytical expression in a uniform medium to approximate the beamwidth, the theoretical basis of this imaging method can be seen as an empirical beam imaging method. Liu and Palacharla (2013) further extended this algorithm to a common-shot migration method.

This paper will first introduce the theory of the Kirchhoff beam migration, and then analyze the impact of the coarse grid on the migration imaging results and illustrate the analysis results by calculating the Marmousi data sets.

1 Methods and principles

This part of the paper will introduce several key steps of Kirchhoff beam migration, including the imaging formula, traveltime calculation and weight function calculation. The implementation flow of Kirchhoff beam migration will be shown at the end of the section.

1.1 Imaging formula

The conventional Kirchhoff migration images each seismic trace (Fig. 1), while the Kirchhoff beam migration images multiple seismic traces in the selected window simultaneously (Fig. 2) (Sun *et al.*, 2000). In the implementation process, Kirchhoff beam migration first needs to divide the seismic records according to different window centers and perform local plane wave decomposition on the seismic data in each window. Finally, each plane wave will be independently imaged and accumulated to obtain the final imaging results (Fig. 3). The imaging formula of the common-shot Kirchhoff beam migration can be expressed as:

$$I_s(x) = \sum_{L_r} \int dp_s \int dp_r A \cdot D_s(L_r, p', \tau') \quad (1)$$

Where L_r represents the windows, p_s is the ray parameter of the center ray emitted by the shot point, p_r is the ray parameter of the center ray emitted by the

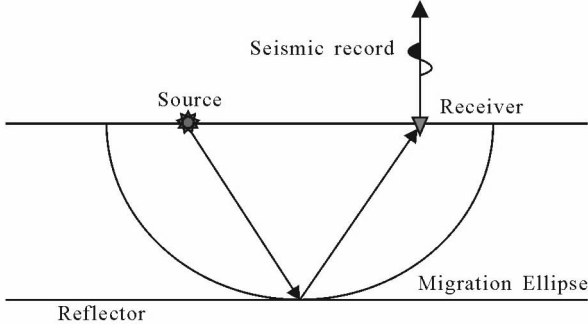


Fig. 1 Imaging method of Kirchhoff migration

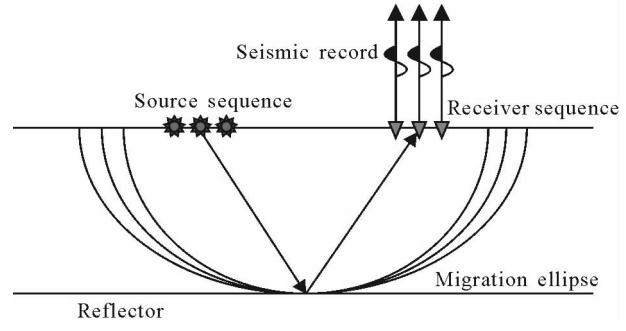


Fig. 2 Imaging method of Kirchhoff beam migration

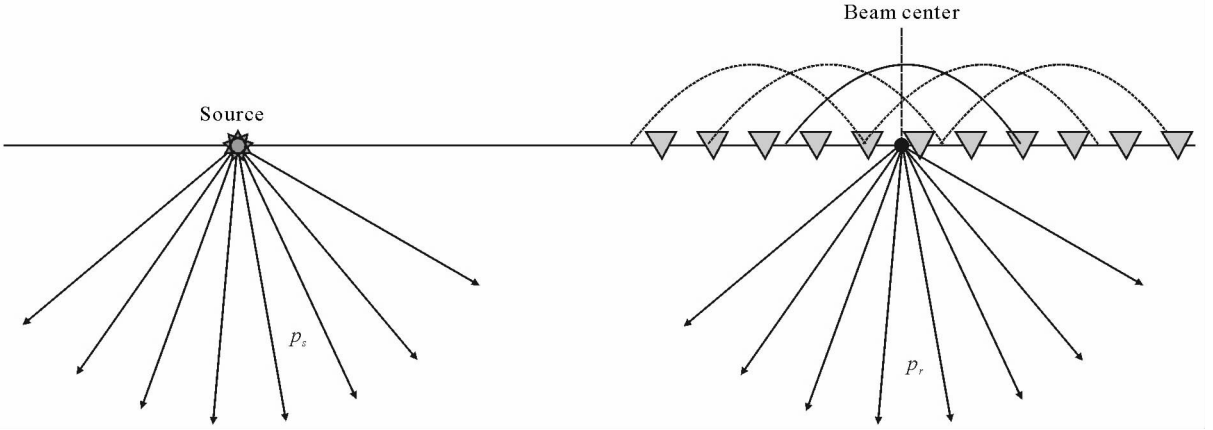


Fig. 3 Schematic diagram of common-shot Kirchhoff beam migration

window center, A is the weight function, D_s is result of local slant stack at the window, the imaging conditions are:

$$p' = p_r \quad (2)$$

$$\tau' = t_s + t_r \quad (3)$$

p' is the slowness which is used for the local slant stack, t_s is the traveltime from the shot point to the imaging point, t_r is the traveltime from the beam center to the imaging point.

1.2 Traveltime calculation

During the implementation of Kirchhoff beam migration, the traveltime information of the grid nodes in the coverage of the beam is obtained by extrapolation of the relevant information on the central ray. As shown in Fig. 4, point x is a grid node covered by the beam, $x_0(x, z)$ is the discrete point on the central ray that is closest to the point, the lateral distance difference between the two points x and x_0 in the Cartesian

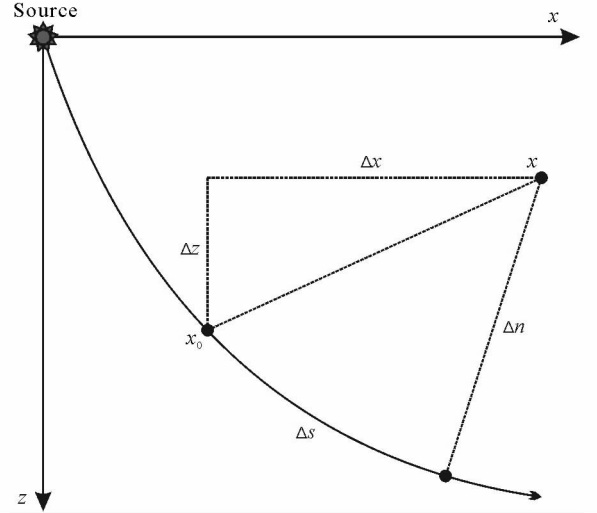


Fig. 4 Schematic diagram of the common-shot Kirchhoff beam migration

coordinate system is Δx , and the longitudinal distance difference is Δz , the distance difference along the ray

path in the ray center coordinate system is Δs , the vertical ray path direction distance difference is Δn . $T(x_0)$ is the traveltime when the center ray reaches point x_0 , $T(x)$ is the traveltime when the beam reaches point x , which can be obtained by the Taylor approximation of the x_0 point traveltime:

$$T(x) \approx T(x_0) + T'(x) + \frac{1}{2}T''(x) \quad (4)$$

$T'(x)$ and $T''(x)$ are the first and second order partial derivatives of $T(x)$ at the center ray coordinate.

1.3 Weight function calculation

Kirchhoff beam migration focuses on rapid imaging of geological structures, and its weight function requirements are not as stringent as other beam migration methods. As shown in Fig. 5, the rays emitted from the shot point is rays, whose angle with the vertical direction is a_s ; the rays emitted from the center of the window is raybc, whose angle with the vertical direction is a_{bc} ; the mapping point of the target imaging point x on the ray rays is x'_s , the distance between point x and point x'_s is n_s , the ray rays are obtained at x'_s by the method described above with a beamwidth of

w_s . The distance from the point x to the mapping point on the ray raybc is n_{bc} , the beam width of the ray raybc at the mapping point of the point x is w_{bc} , and the weight function at the point x can be expressed by the following formula:

$$A = \cos^2 \left[\frac{\pi}{4} (n_s^2 w_s^{-2} + n_{bc}^2 w_{bc}^{-2}) \right] \cos[0.5 \times (a_s - a_{bc})] \quad (5)$$

The purpose of the $\cos[0.5 \times (a_s - a_{bc})]$ term added in equation (5) is to attenuate the effect of critical reflection energy on the migration imaging.

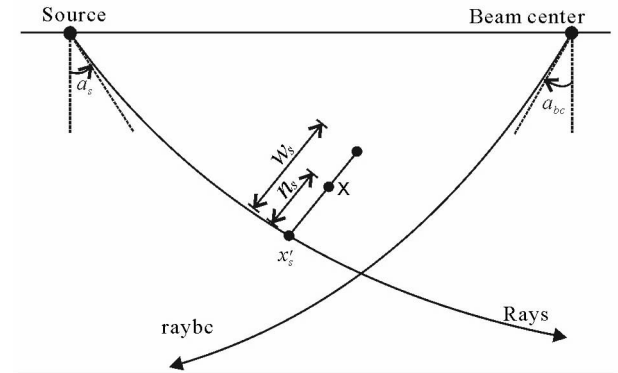


Fig. 5 Schematic diagram of weight function calculation method

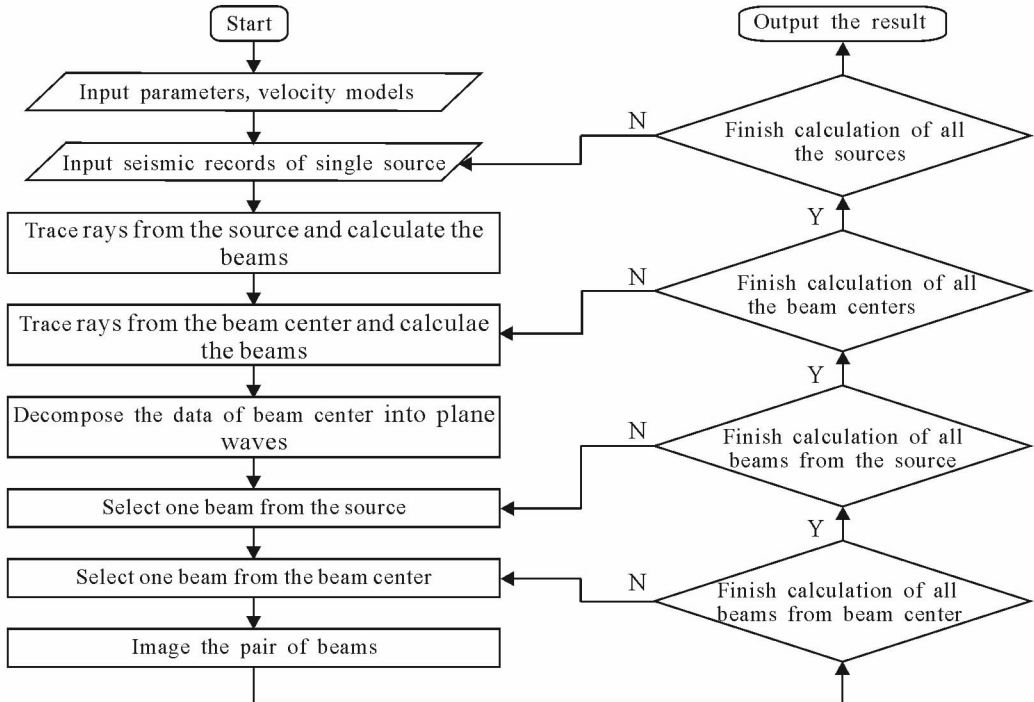


Fig. 6 Implementation flow chart of common-shot Kirchhoff beam migration

1.4 Algorithm flow

The implementation of Kirchhoff beam migration can be divided into three steps: the first step is to divide the seismic record into different local regions; the second step is to decompose the seismic records into plane waves in different directions; the third step is to image the plane waves in different directions. The implementation of the common-shot Kirchhoff beam migration is shown in Fig. 6.

2 Coarse grid selection

In this part, the coarse grid selection which have a great influence on the imaging effect of Kirchhoff beam migration are discussed. Some selection criteria are given, and the influence of this parameter on the migration imaging is verified by the numerical model.

During the implementation of Kirchhoff beam migration, when calculating the information of the grid nodes covered by the beam, if the calculation is performed for each grid node, it will inevitably reduce the calculation efficiency. In this paper, the coarse grid technique in Gaussian beam migration imaging (Hale, 1992; Yue *et al.*, 2011) is adopted in Kirchhoff beam migration to improve computational efficiency. Considering that the traveltime and weight function in the beam are monotonous, Kirchhoff beam migration also satisfies the application conditions of the coarse grid. In the application process, the information of the grid nodes on the coarse grid is first calculated, and then when the information on the fine grid nodes is calculated, the information is inserted through the coarse grid points' information (Fig. 7). This progress can greatly reduce the time of Kirchhoff beam migration.

The application of coarse grid technique has a significant improvement in the computational efficiency of Kirchhoff beam migration, but it is worth noting that the application of coarse grid technique should not reduce the quality of migration imaging. Generally, the larger the mesh, the less the calculation time of the entire migration algorithm, but if the coarse grid is too large, it will affect the calculation accuracy of

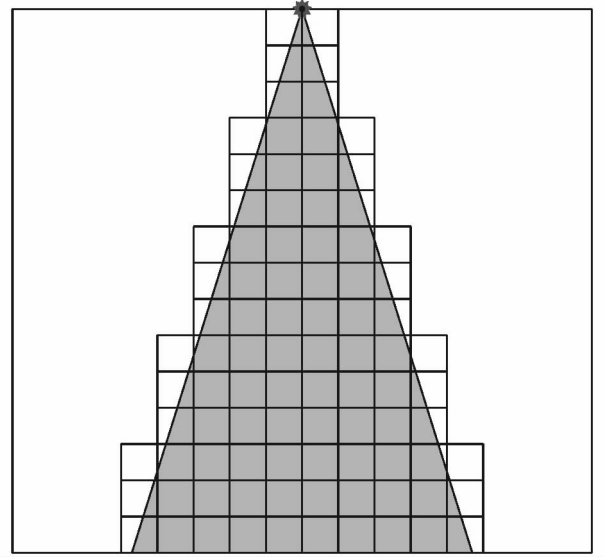


Fig. 7 Schematic diagram of coarse grid

the attribute information of grid nodes, and may reduce the final migration imaging effect.

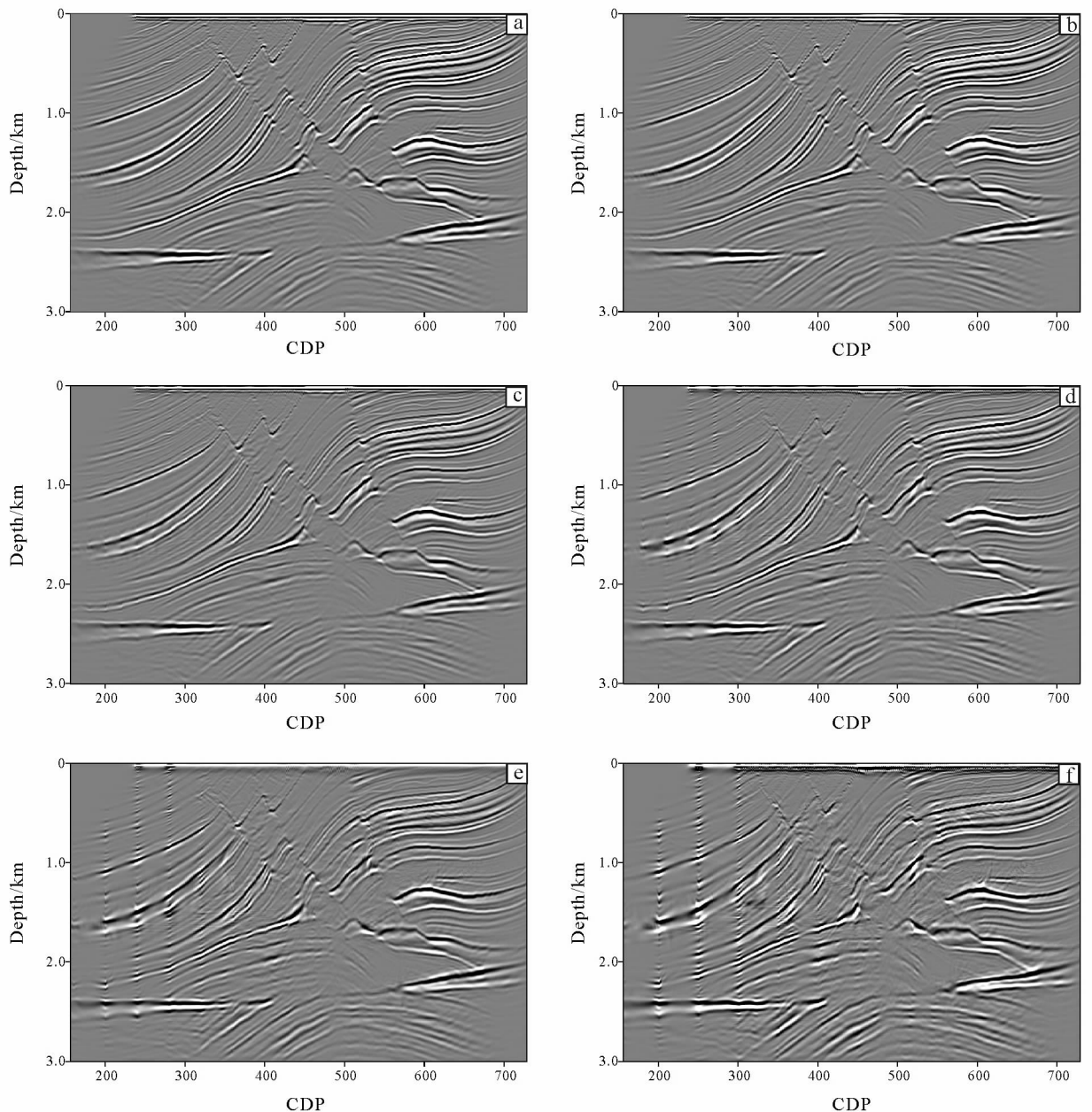
3 Numerical experiment

This section will adopt the Marmousi data sets to verify the effect of the coarse grid selection on Kirchhoff beam migration. Figure 8 shows the results of Kirchhoff beam migration for the Marmousi model corresponding to different coarse grid. The expansion ratios of the fine mesh corresponding to Fig. 8 are respectively 5 times, 10 times, 20 times, 30 times, 40 times and 50 times.

Observing the migration result, it can be found that when the mesh magnification is 5 times and 10 times, the migration result is better. When the coarse grid continues to expand to 20 times, the left part of the migration section is discontinuous. In the case where the coarse grid is further expanded to 30 times, the discontinuity of the left part in the migration section is more serious. When the migration coarse grid is further expanded to 40 times, at this time, in addition to the discontinuity problem in the left part, the suppression of the migration noise is also deteriorated, and the signal-to-noise ratio of the entire migration section is decreased. When the migration coarse grid is expanded to 50 times, the discontinuity in the migration section

is serious, and the migration noise is higher, which is enough to affect the appearance of the geological struc-

ture in the migration profile, and some fine structures (Such as faults) are difficult to identify.



The fine meshes are expanded to different times: (a) = 5 times; (b) = 10 times; (c) = 20 times; (d) = 30 times; (e) = 40 times; (f) = 50 times.

Fig. 8 Results of Kirchhoff beam migration for Marmousi models corresponding to different coarse grids

4 Conclusion

When applying coarse grid technique in Kirchhoff beam migration, the coarse grid should be as larger as possible without affecting the final migration result.

The larger the coarse grid is, the higher the calculation efficiency of the beam migration is. However, if the coarse grid is too large, the errors of important attribute information such as the traveltimes and weight function of the grid node will be larger, which will re-

duce the final migration imaging effect and affect the identification of geological structures. Meanwhile, the selection of coarse grid is related to the size of the model, the distribution of the observation system, the complexity of the model, etc. The grid size range of the Kirchhoff beam migration is usually from 100 – 300 m, which is 5 –15 times of the fine grid.

References

- Červený V, Popov M M, Pšenčík I. 1982. Computation of wave fields in inhomogeneous media—Gaussian beam approach. *Geophysical Journal of the Royal Astronomical Society*, **70**(1) : 109-128.
- French W S. 1975. Computer migration of oblique seismic reflection profiles. *Geophysics*, **40**(6) : 961-980.
- Gray S H. 2005. Gaussian beam migration of common-shot records. *Geophysics*, **70**(4) : S71-S77.
- Hagedoorn J G. 1954. A process of seismic reflection interpretation. *Geophysical Prospecting*, **2**(2) : 85-127.
- Hale D. 1992. Computational aspects of Gaussian beam migration. DOI: 10.2172/7200248
- Hale D. 1992. Migration by the Kirchhoff, slant stack, and Gaussian beam methods. DOI: 10.2172/7115487
- Hill N R. 1990. Gaussian beam migration. *Geophysics*, **55**(11) : 1416-1428.
- Hill N R. 2001. Prestack Gaussian-beam depth migration. *Geophysics*, **66**(4) : 1240-1250.
- Liu J, Palacharla G. 2011. Multiarrival Kirchhoff beam migration. *Geophysics*, **76**(5) : WB109-WB118.
- Liu J, Marcinkovich C. 2013. Shot-profile Kirchhoff beam migration//83th Annual International Meeting, SEG Expanded Abstracts.
- Nowack R L, Sen M K, Stoffa P L. 2003. Gaussian beam migration for sparse common-shot and common-receiver data//73th Annual International Meeting, SEG Expanded Abstracts.
- Schneider W A. 1978. Integral formulation for migration in two and three dimensions. *Geophysics*, **43**(1) : 49-76.
- Sun Y, Qin F, Checkles S, *et al.* 2000. 3-D prestack Kirchhoff beam migration for depth imaging. *Geophysics*, **65**(5) : 1592-1603.
- Xu S, Lambare G, Calandra H. 2004. Fast migration/inversion with multivalued ray fields: Part 2—applications to the 3D SEG/EAGE salt model. *Geophysics*, **69**(5) : 1320-1328.
- Xu S, Lambare G. 2004. Fast migration/inversion with multivalued ray fields: Part 1—method, validation test, and application in 2D to Marmousi. *Geophysics*, **69**(5) : 1311-1319.
- Yue Y B, Li Z C, Zhang P, *et al.* 2010. Prestack Gaussian beam depth migration under complex surface conditions. *Applied Geophysics*, **7**(2) : 143-148.